LINKING SCALES IN FRACTURE MECHANICS

John W. Hutchinson
Division of Engineering and Applied Sciences, Harvard University
Cambridge, MA 02138, USA

ABSTRACT

A overview is given of fracture mechanics models which incorporate a description of the near–tip fracture process. Emphasis is on applications to metals and interfaces between metals and ceramics where plastic flow makes a substantial contribution to toughness and crack growth resistance. Important scaling distinctions emerge between computational models for fracture taking place by void nucleation, growth and coalescence and those characterizing cleavage or decohesion.

KEYWORDS

Fracture models, crack tip stresses, crack growth resistance, metal–ceramic interfaces.

1. INTRODUCTION

Linking the macroscopic scale to the microscopic scale to gain basic understanding and quantitative models of fracture properties goes back to the earliest days of fracture mechanics, as exemplified by Griffith's work on the fracture of glass. Nevertheless, much of the great success of fracture mechanics as an engineering subject rests on tests, as opposed to models at the microscopic scale, to obtain essential fracture properties such as toughness, crack growth resistance, and fatigue crack growth rates. Linear elastic fracture mechanics (LEFM) provides a framework for taking material data from test specimens to assess the residual strength or load cycles to failure of a cracked structure or component. The central idea underlying LEFM is Irwin's notion of an autonomous region at the crack tip characterized by the elastic stress intensity factor and subsuming all nonlinear behavior, including the fracture process. In LEFM, details of the exterior geometry and loading are felt only through the history of the stress intensity factor, K. LEFM breaks down and nonlinear fracture mechanics comes into its own when zone of nonlinearity ceases to be contained within the K–field. This can happen when the fracture process zone itself becomes too large, as in the case of extensive micro–cracking at a macroscopic crack in a polycrystalline ceramic, or it can result when the fracture process zone remains small but the surrounding plastic zone becomes large. This latter situation, labeled large scale yielding in elastic–plastic fracture mechanics, has received considerable attention over the past several decades, with mixed success.

Until recently, the main approach to extending LEFM into the large scale yielding regime has been to use elastic–plastic crack solutions and to invoke an autonomous zone at the crack tip controlled by the J–integral. This is the natural extension of Irwin's idea for LEFM, requiring the fracture process zone to be embedded within a crack tip field uniquely characterized by J. While this approach can be used under restricted conditions and it has had some notable successes, its limitations are equally apparent and have been well exposed in the technical literature (e.g., Broberg, 1995). Even for the initiation of growth of stationary cracks, the notion of a near–tip field uniquely tied to J breaks down because of the strong influence of outer geometry and loading conditions on the level of hydrostatic tension at the tip. Hydrostatic tension has a significant influence on fracture initiation, whether the process be the ductile mechanism of void nucleation, growth and coalescence or cleavage. The absence of a unique characterizing parameter for the crack tip field carries over to the description of crack growth resistance. Moreover, the J–integral is based on a deformation theory formulation of plasticity which is not applicable if extensive amounts of crack growth take place. While further progress and understanding has been achieved on the basis of a two–parameter crack tip mechanics (Hancock *et al.*, 1993), it has been apparent for some time that the fracture process must be directly incorporated into the mechanics if it is to be widely applicable to tough, ductile structural metals.

A nonlinear fracture mechanics for ductile fracture under small or large scale yielding has recently emerged based on computational formulations which embed a model of the fracture process within an outer continuum elastic–plastic description. These formulations permit direct calculation of crack initiation and advance. The inputs to the models are microstructural parameters such as void nucleation strains, volume fraction of void nucleating particles, etc. In practice, the choice of these parameters is made to reproduce one or more sets of specimen test records for the material in question. In this sense, calibration of the models is intended to remain strongly tied to test data, as has exemplified engineering fracture mechanics from its beginnings. The new nonlinear fracture mechanics has been made possible by the development and verification of mechanistically–based models of void growth, on the one hand, and by the increases in computational power made widely available in recent years. It has become feasible to routinely perform computations which span the scale from the structure or component (on the order of a meter) down to the scale of the void growth fracture process (on the order of tens of microns). The development of computational models for ductile fracture was first pursued in France (Rousselier, 1987; Rousselier *et al.*, 1989) and with paralleling work in England (Bilby *et al.*, 1993; Li *et al.*, 1994), Denmark (Tvergaard and Needleman, 1984), Germany (Brocks *et al.*, 1995; Sun *et al.*, 1992) and the United States (Needleman and Tvergaard, 1987; Shih and Xia, 1995; Xia and Shih, 1995; Xia *et al.*, 1995). An illustration of the predictive capability of the models will be given later in this article.

The scale of the void growth fracture process for most structural metals lies within the range, typically, from several microns to as much as one hundred microns. By contrast, when the process is atomic cleavage or decohesion of a metal/ceramic interface, the scale of the fracture process is on the order of angstroms. The fracture of interfaces is currently of considerable interest in the physics community where computations of interface separation energies using atomistic methods are being extended and refined. There is also considerable technological interest in metal/ceramic interfaces, and extensions of linear and nonlinear fracture mechanics applicable to such systems have been developed. Efforts to link the atomistic results to macroscopic fracture measures such as interface toughness requires that scales on the order of angstroms to centimeters be spanned. The expanded scale introduces two challenges not encountered in modeling fracture controlled by the void growth process. One is simply the computational difficulty of spanning the extreme range of scales. The second, which will be highlighted here, is the inadequacy of conventional continuum plasticity at scales below several microns. The atomic decohesion process is "screened" from the applied loads by plasticity. As has long been appreciated, plasticity contributes mightily to the macroscopic toughness of strong interfaces.

This overview is organized to bring out the some of the progress and challenges involved in linking to the fracture process from the macroscopic scale. The viewpoint is of one who has been motivated primarily to develop fracture mechanics for engineering applications. In other words, this article puts the main emphasis on crossing the bridge from the macroscopic side of gulf, rather that the other way around. Section 2 discusses a generic model which employs an embedded traction–separation law to characterize local material failure. The model is used to bring out some of the issues mentioned above for the two major fracture processes, void growth and atomic decohesion. Section 3 reviews the new fracture mechanics for ductile structural metals. Section 4 addresses problems alluded to above when the fracture process occurs at the atomic scale. Specifically, the importance of establishing the link through the scales is discussed, and recent attempts to extend the characterization of crack tip fields to smaller scales using new plasticity models will be reviewed.

2. EMBEDDED PROCESS ZONE (EPZ) MODEL

The EPZ model for mode I, plane strain cracks (Tvergaard and Hutchinson, 1992) anticipates that crack growth will occur as an extension of the existing crack plane and employs a traction–separation relation as a internal boundary condition along the extended crack plane to model the fracture process. The separation law, $\sigma(\delta)$, which is shown in Fig. 1, is characterized by the work of separation per unit area, $\Gamma_0 = \int_0^{\delta_c} \sigma(\delta)d\delta$, the peak separation stress, $\hat{\sigma}$, and shape factors, λ_1 and λ_2, which are of secondary importance. The material off the extended crack plane is taken to be a conventional elastic–plastic solid. For the case of an isotropic elastic–plastic solid, the J_2 flow theory is used which is specified by the elastic Young's modulus and Poisson's ratio, E and ν, the tensile yield stress, σ_Y, and the strain hardening index, N (with $N = 0$ coinciding with an elastic–perfectly plastic solid). The separation δ is identified with the displacement jump across the extended crack plane.

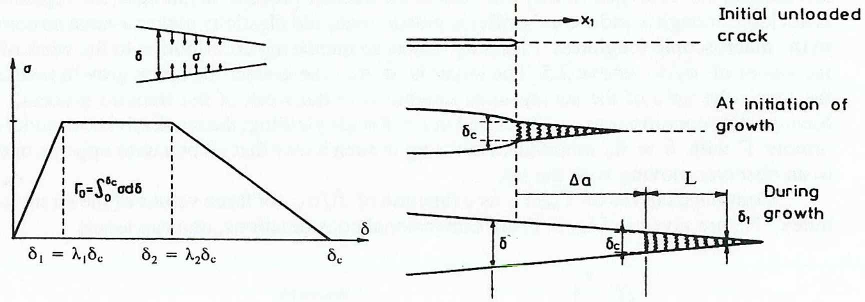

Figure 1. Traction–separation law of the fracture process and details at the crack tip.

Initiation of growth is identified with attainment of δ_c at the tip, and the tip is advanced when conditions are such that δ is maintained at δ_c. No further conditions need be specified. The length L of the fracture process zone at any stage of loading is not known but must be determined as part of the solution process. The model is computationally intensive in that predictions require a finite element representation of the solid, finely meshed in the crack tip region. Applied loads and external geometry are represented in the usual manner. In general, there is no distinction between large and small scale yielding, however, small scale yielding is readily modeled if the outer elastic field is prescribed to be the classical K–field. The interaction between the fracture process and the surrounding plastic zone is the essential feature captured by the model. This interaction is exceptionally nonlinear, as will be brought out in the sequel. It is intended that the model be generic in that it sheds light on more that one fracture process. Indeed, it will be seen that work of the fracture process Γ_0 is typically on the order of thousands of Joules when the fracture mechanism is void growth, while it is on the order of one Joule when atomic decohesion governs.

Assuming the loading is monotonic prior to initiation of crack growth, the plastic deformation will be nearly proportional and a deformation theory representation is a good approximation. The J–integral is path–independent, and its application to initiation of growth when the condition $\delta = \delta_c$ is first attained at the tip gives $J = \Gamma_0$. Thus, according to the model, the work of the fracture process is also the critical value of J corresponding to initiation.

Consider application of the model to small scale yielding conditions where the crack can be regarded as being semi–infinite and the remote field is specified to be the K–field. Let

$$\Gamma = \frac{(1 - \nu^2)K^2}{E} \tag{1}$$

be the measure of the applied loading such that for integration contours in the elastic region surrounding the plastic zone, $J = \Gamma$. Following Tvergaard and Hutchinson, define a reference plastic zone size by

$$R_0 = \frac{E\Gamma_0}{3\pi(1 - \nu^2)\sigma_Y^2} \tag{2}$$

This length quantity can be interpreted as an estimate of the half–height of the plane strain plastic zone *if the applied loading satisfies* $\Gamma = \Gamma_0$. Computed curves of Γ/Γ_0 versus normalized crack advance, $\Delta a/R_0$, are shown in Fig. 2 for a set of representative nondimensional material parameters. As already noted, initiation occurs when $\Gamma = \Gamma_0$. If the ratio of peak separation stress to tensile yield stress, $\hat{\sigma}/\sigma_Y$, is less than about 2.5, no crack growth resistance occurs, and the crack advances at the level specified by the work of the fracture process. In this case, the separation stress is not large enough to induce a significant plastic zone, and plasticity makes almost no contribution to the macroscopic toughness. Plasticity makes an increasing contribution to the work of fracture for values of $\hat{\sigma}/\sigma_Y$ above 2.5. The larger is $\hat{\sigma}/\sigma_Y$, the greater the crack growth resistance and the larger the ratio of the steady–state toughness to the work of the fracture process, Γ_{ss}/Γ_0. Steady–state conditions are well defined in small scale yielding: the crack advances under constant remote Γ with $\delta = \delta_c$ maintained at the tip in such a way that all behavior appears unchanging to an observer moving with the tip.

Computed curves of Γ_{ss}/Γ_0 as a function of $\hat{\sigma}/\sigma_Y$ for three values of the strain hardening index, N, are given in Fig. 3. From dimensional considerations, one can assert

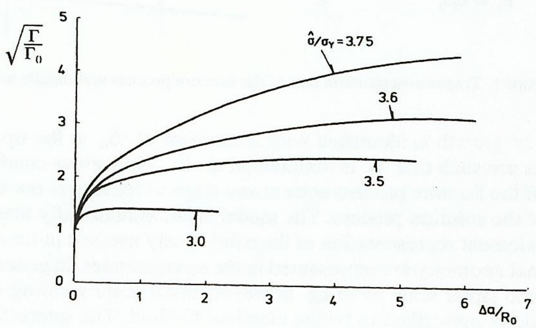

Figure 2. Crack growth resistance curves in small scale yielding from Tvergaard and Hutchinson (1992). ($N = 0.1$, $\lambda_1 = 0.15$, $\lambda_2 = 0.5$, $\sigma_Y/E = 0.003$).

$$\frac{\Gamma_{ss}}{\Gamma_0} = F\left[\frac{\hat{\sigma}}{\sigma_Y}, N, \frac{\sigma_Y}{E}, \nu, \lambda_1, \lambda_2\right] \tag{3}$$

but dependence on all but $\hat{\sigma}/\sigma_Y$ and N is relatively unimportant. The plasticity contribution to the total work of fracture is reflected by the extent to which Γ_{ss} exceeds Γ_0, which is considerable when $\hat{\sigma}/\sigma_Y$ becomes sufficiently large. Indeed, the contribution of plastic dissipation in the plastic zone to macroscopic work of fracture can be many times the work of the fracture process, yet, by (3), Γ_{ss} nevertheless scales with Γ_0. Nonlinear amplification of the work of the fracture process by the plasticity zone is made explicit by the model, and is evident in the trends of Fig. 3.

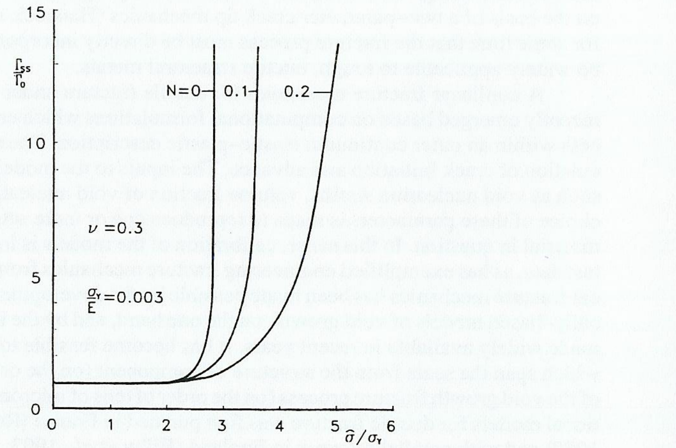

Figure 3. Ratio of macroscopic steady–state toughness to work of the fracture process from Tvergaard and Hutchinson (1992). ($\lambda_1 = 0.15$, $\lambda_2 = 0.5$, $\sigma_Y/E = 0.003$).

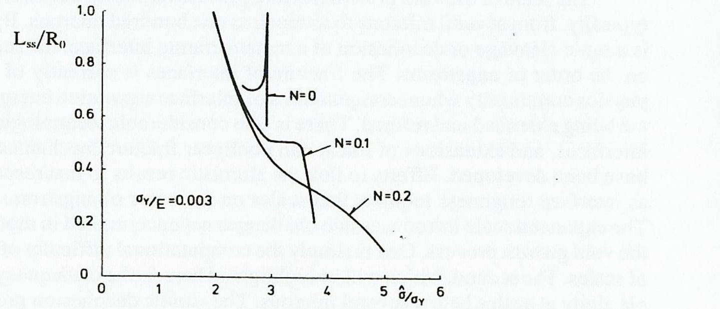

Figure 4. Normalized length of the fracture process zone in steady–state growth from Tvergaard and Hutchinson (1992). ($\lambda_1 = 0.15$, $\lambda_2 = 0.5$, $\sigma_Y/E = 0.003$).

The computed length of the fracture process zone in steady–state growth, L_{ss}, is plotted in Fig. 4 as L_{ss}/R_0. The process zone length is taken as the distance from the tip where $\delta = \delta_c$ to the point where the peak stress is first attained at $\delta = \lambda_1\delta_c$. The plastic zone half–height, R_p, is given approximately by $R_p = (\Gamma_{ss}/\Gamma_0)R_0$, and thus it can be seen that L_{ss}/R_p drops sharply as $\hat{\sigma}/\sigma_Y$ increases. Broberg (1995) has suggested that the ratio, $B = R_p/L_{ss}$, is a good measure of the extent to which the fracture process is embedded within the surrounding plastic zone and the degree to which plastic dissipation is expected to contribute to the total work of fracture. The larger is B, the greater the plasticity contribution to toughness relative to that from the fracture process.

3. CRACK GROWTH MODELS FOR THE MECHANISM OF VOID GROWTH

The EPZ model can be specialized to the case where the fracture mechanism is void nucleation, growth and coalescence, as has been done by Tvergaard and Hutchinson (1992, 1994, 1996). To do so requires that the parameters characterizing the traction–separation law, $\hat{\sigma}$ and Γ_0, must be related to parameters of the actual fracture process, such as nucleation strain, initial void volume fraction, f_0, and void spacing D. This can be done with the aid of a micro–mechanical model of void growth such as that due to Gurson (1977). The ratio $\hat{\sigma}/\sigma_Y$ is a strong function of f_0, decreasing as f_0 increases. The work of the fracture process required to separate a localized plane of voids is relatively independent of f_0, depending primarily on the thickness of the band, which scales with D. To a reasonable approximation (see full details in cited papers), it is found that

$$\Gamma_0 = \frac{1}{2}\sigma_Y D \qquad (4)$$

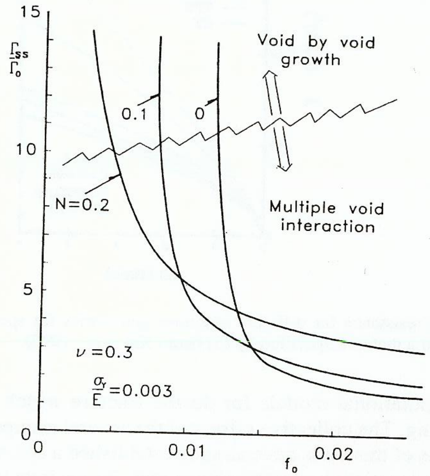

Figure 5. Ratio of the total work of fracture in steady–state to the work of the fracture process when void growth and coalescence is the fracture mechanism. (From Tvergaard and Hutchinson, 1996).

The outcome of this specialization is shown in Fig. 5, where the results from Fig. 3 are replotted directly in terms of f_0 for the case where voids are present in the undeformed material. The total work of fracture of a tough material $(f_0 < 0.005)$ will largely be due to the dissipation in the plastic zone surrounding the plane of localized and coalescing voids. Note that substantial plastic dissipation is involved in the fracture process itself, as is evident from (4). Indeed, typical values from (4) for Γ_0 would fall in the range from 1KJoule to 100KJoule, with plastic deformation constituting a large part of the work of the fracture process.

To be valid, the specialization requires that the predicted length of the fracture process zone, L, be large compared to the spacing between the voids, D. This is a consistency condition dictated

by the fact that the computation of $\hat{\sigma}$ and Γ_0 in terms of f_0 assumes the fracture process is a localized plane of voids ahead of the tip. Consistency breaks down for levels of Γ_{ss}/Γ_0 above about 10, as indicated in Fig. 5. In this range, the model predicts that L is on the order of D suggesting that crack tip advances "void to void" rather than by inducing a localized plane of interacting voids strung out ahead of the tip. Thus, there are two distinct regimes governing ductile fracture. The EPZ model is not valid in the "void to void" regime, at least as it is formulated above. The new models for ductile fracture mentioned in the Introduction encompass both regimes because they incorporate voids as discrete entities. These are now discussed.

The new models (c.f. references cited in the Introduction) have been developed as tools for engineering fracture analysis, with provisions for calibration against test data for specific materials under prescribed environmental conditions. All of the models are formulated within a finite element framework, employing special void–containing elements ahead of the crack tip. For mode I, the plane of crack growth has been anticipated to be the extended plane of the crack in most of the formulations pursued to date, but this restriction can be lifted (Needleman and Tvergaard, 1987). The models assume the voids are discrete entities with absolute size and spacing. Equivalently, void size and spacing can be specified by void volume fraction, f, and spacing, D, and these will be two of the fracture process parameters used in the present discussion. In nearly all the model formulations, one void per element is assumed such that the element size is directly tied to D. Only within recent years has computing power been sufficient to allow routine calculations where, to link scales, the mesh size at the crack tip is on the order of 10 to 100 microns while outer boundary dimensions are on the order of 1 to 10 centimeters.

Void damage in the elements ahead of the crack tip evolves according to specified rules which characterize the local multi–axial constitutive relation. It is the parameter set of this constitutive relation which must be calibrated against actual fracture data to produce a quantitatively reliable crack growth model. Two constitutive relations based on void growth have been used for the embedded damage elements. The Rousselier Model (Rousselier, 1987) has been employed in the model used by the French and English groups, while the Gurson Model (1977) has been employed in the other crack growth models. Both models employ an initial void volume fraction, f_0, and D as primary parameters, along with additional parameters such as strains characterizing void nucleation and void coalescence.

In the work on specific materials carried out by the French and English researchers, initial values of the damage parameters have been chosen such that the model reproduces fracture data taken on notched bars designed to cover a range of stress triaxialities. To some extent, the parameters have also been directly related to microstructural features such as the size and spacing of void nucleating particles. The validity of the crack growth model has been demonstrated by employing it to predict crack growth histories and associated load–deflection behavior of a variety of fracture specimen of the same material.

The approach of the German and American work parallels that of the French in most respects. However, instead of using notch bar data to calibrate the damage elements, these workers choose f_0, D and other parameters such that their models fit crack growth data taken from laboratory test specimens. While perhaps not as fundamental, this approach has the merits of calibrating against data representative of the intended application of the model. In any case, either approach is feasible for both sets of models.

Much of the motivation for the development of these new models has come from the nuclear power industry where problems related to cracking of pressure vessels and piping remain in need of further clarification and quantification. In several of these problems, such as the thermal shock of a reactor pressure vessel, the thickness of the section leads to a cracking problem which falls within the category of small scale yielding, or, perhaps, intermediate scale yielding. However, residual strength assessment requires consideration of reasonably large amounts of crack growth, well beyond what can be obtained from laboratory test specimens. Moreover, resistance curve data taken from laboratory specimens is invariably large scale yielding data, and therefore crack tip triaxiality variation comes into the picture with its strong effect on crack growth behavior. The new models appear to be able to successfully deal with the two problems which have plagued the development of a nonlinear fracture mechanics for tough ductile materials: variable crack tip triaxiality and extensive amounts of crack growth. Once the parameters of the model are established for a given material, crack growth initiation and resistance are computed, as are the histories of load, deflection and crack stability.

The new models have been applied to several large scale problems from the power industry, as cited in some of the references listed in the Introduction. Here, we will illustrate their application to predict the dependence of crack growth behavior on size and geometry of test specimens (Xia *et al.*, 1995). In all of the examples, the constitutive parameters characterizing the material are chosen to be

$$E = 200\,\mathrm{GPa} \quad , \nu = 0.3 \quad , N = 0.1 \quad ,$$
$$\sigma_Y = 400\,\mathrm{MPa} \ , \ f_0 = 0.005 \ , \ D = 200\,\mu\mathrm{m} \qquad (5)$$

This set produces predictions representative of experimental data taken from fracture specimens for a tough pressure vessel steel (A533B).

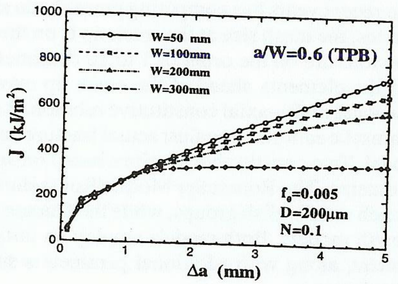

Figure 6. The effect of specimen size of crack growth resistance as predicted for three–point bend specimens of a material specified by (5) (from Xia *et al.*, 1995).

Fig. 6 shows predictions on the effect of specimen *size* on crack growth resistance (J vs. crack advance Δa) for three–point bend specimens of width W and initial crack length a_0. In all four specimens, a_0/W is fixed at 0.6 and thus the specimens can be regarded as deeply cracked. The deeply cracked three–point bend specimen is generally regarded as possessing high crack tip triaxiality (see Fig. 7 below). The specimens are identical in all respects except size. The J–integral has been evaluated on a contour taken near the outer boundary. Traditionally, J has been a convenient measure of the applied load and will be used for this purpose here, even though one would almost certainly bypass use of J in an actual application. The loss of path–independence of the J–integral on contours taken near the tip is not at issue here. The lowest curve in Fig. 6 for $W = 300$ mm coincides with the result from an independent calculation under small scale yielding. (To make contact with the EPZ model of the previous section, note that $\Gamma_0 = 40\,\mathrm{KJ/m^2}$, from (4) and (5). Based on the lower curve in Fig. 6, Γ_{ss}/Γ_0 is about 8). The smaller specimens display increasing amounts of large scale yielding as the load is increased. The remaining ligaments of the smaller specimens have fully yielded well before 1mm of growth has occurred. For growth up to about 1mm there is almost no size dependence of the crack growth resistance. For Δa above 1mm, the discrepancy becomes significant with smaller specimens displaying higher resistance than larger specimens. Note that this trend is displayed by specimens believed to have roughly similar levels of crack tip triaxiality. Its implication for any approach based on analysis

using J resistance curve data is disturbing in that it suggests that data taken from small specimens which is applied to predict the behavior of larger components will *overestimate* resistance to crack advance.

The effect of different geometries is shown in Fig. 7, again for the material specified by (5). The five geometries are compact tension (CT), three–point bend (TPB), single edge–notched tension (SENT), double edge–notched tension (DENT), and center cracked panel (CCP). The full range of crack tip triaxiality is generated by specimens of these geometries, from highest (CT) which is thought to be close to that for small scale yielding to lowest (CCP). The width W (or half–width for the DENT and CCP) of each specimen is the same ($W = 5.08$ cm), and the initial crack length (or half–crack length for the CCP) is chosen such that $a_0/W = 0.6$. The J–integral is again evaluated on a contour remote from the crack tip. Each specimen is well into the large scale yielding range once crack growth is underway. The associated load–deflection curves reach a maximum after about 1 to 2 mm of crack growth, depending on the particular specimen. The strong dependence on specimen geometry displayed in Fig. 7 replicated experimental trends quite faithfully (Xia *et al.*, 1995). Similar trends have been computed by each of the groups with their respective models.

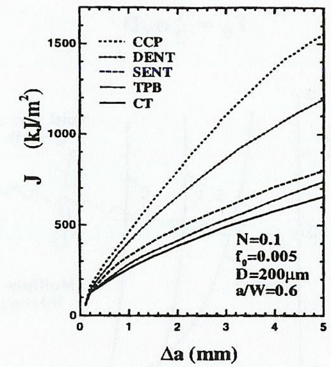

Figure 7. Crack growth resistance for different specimen geometries for specimens of nominally the same size ($W = 5.08$ cm) made of a material specified by (5) (from Xia *et al.*, 1995).

The new computational models for ductile fracture which incorporate damage elements appear most promising. The collective efforts of the several groups in various countries involved in developing models of this class have already established a convincing case for their predictive power and for their potential as an engineering tool. Extensions to cope with crack advance out of the initial crack plane are possible but will require considerable additional work. The effect of shear localization, which becomes increasingly important in very high strength steels, will be particularly challenging. One important application which appears feasible without major innovation is the three dimensional problem of an elliptical surface crack in a think plate undergoing combinations of bending and stretching. This problem would be a good test for the models because stress triaxiality varies along the crack front, producing crack shape changes as the crack advances.

4. SOME CHALLENGES FACING THE DEVELOPMENT OF CRACK GROWTH MODELS FOR DECOHESION AT THE ATOMIC SCALE

Cleavage cracking in structural steels ultimately involves separation across cleavage planes at the atomic scale, but this scale does not appear to control macroscopic cracking. Initiation of cleavage in a structural steel is usually triggered by an event on the scale of brittle second phase particles (typically, microns to tens of microns). The brittle particles crack thereby nucleating running microcracks which coalesce with the main crack producing extension. The macroscopic cleavage toughness of a relatively tough steel can be on the order of several KJ/m^2. Plasticity makes a huge contribution to the toughness since the atomistic work of cleavage of the lattice in the absence of any plasticity is only on the order of one J/m^2. In a polycrystalline structural steel, part of the plastic dissipation arises in the plastic zone surrounding the tip, and another part results from the plastic deformation involved in tearing uncleaved ligaments bridging the two fracture surfaces. The scale which seems to control macroscopic cleavage cracking of structural steels is thus on the order of the spacing between second phase particles and the grain size. Computational engineering models for initiation, growth and arrest which link to these scales are not as far advanced as those for the void growth mechanism.

In this overview, we will focus on systems where macroscopic fracture is controlled at the atomic level. Specifically, we will highlight efforts to link macroscopic toughness through the plastic zone down to the scale of atomic decohesion.

In a remarkable series of experiments, Elssner *et al.* (1994) measured both the macroscopic fracture toughness, Γ_{ss}, and the atomic work of separation, Γ_0, of an interface between a single crystal of niobium and a sapphire single crystal. The macroscopic work of fracture was measured using a four–point bend specimen designed for the determination of interface toughness, while the atomistic value was inferred from the equilibrium shapes of microscopic pores on the interface. The crystals were diffusion bonded, and tests on more than one relative crystal orientations were performed. The interface between the two materials, which was fully characterized, remained atomistically sharp. In addition, experiments were conducted on specimens containing a small amount of segregant of another element on the interface for the purpose of exploring its effect on the atomistic and macroscopic work of fracture. Data for two of the interfaces are presented in Table I, one without a segregant and one with a fractional atomic layer of silver.

Atomistic (Γ_0) and Macroscopic (Γ_{ss}) Work of Nb/Al_2O_3 Interface Fracture

Interface with no segregant :	$\Gamma_0 = 1.0 \pm 0.2\,Jm^{-2}$	$\Gamma_{ss} = 2100\,Jm^{-2}$
Interface with Ag segregant :	$\Gamma_0 = 0.6 \pm 0.2\,Jm^{-2}$	$\Gamma_{ss} = 400\,Jm^{-2}$

The values for Γ_0 are representative of the atomistic separation energy of most metal/ceramic interfaces, i.e. on the order of $1\,Jm^{-2}$. The macroscopic interface toughnesses are representative of an interface where the metal undergoes plastic deformation in the vicinity of the crack tip. In the case of all the Nb/Al_2O_3 crystal pairs, the separation occurred cleanly down the interface with no remnant of either material left on the surface of the other. The two observations relevant to this overview are (a) the huge ratio of Γ_{ss} to Γ_0 and (b) the five–fold drop in the macroscopic toughness brought about by the 40% reduction in Γ_0 due to the segregant. These experiments provide a striking illustration of the way plasticity magnifies the work of fracture process when that process is at the atomic or molecular scale and the interface is strong. They also emphasize just how extraordinarily nonlinear is the coupling between the work of the fracture process and the macroscopic work of fracture through the plastic zone: a relatively small reduction in the strength of the interface parlays into a huge reduction in the macroscopic work of fracture.

The EPZ Model captures some of the qualitative aspects of the link to the scale of the fracture process for such systems, but the model clearly falls short from a quantitative standpoint. Most notably, the maximum stress levels which can be achieved ahead of the crack tip according to the EPZ Model (which, it should be recalled, is based on conventional plasticity) is not greater than about 4 to 5 times the tensile yield stress σ_Y of the metal, depending somewhat on strain hardening. This is evident from the plots in Fig. 3 for mode I growth in a homogeneous material, which are also representative of results from the EPZ Model for metal–ceramic interfaces (Needleman (1987); Tvergaard and Hutchinson (1993); Wei and Hutchinson (1996a)). The stress levels needed to produce atomic decohesion of a lattice or a strong interface are generally considerably larger than $5\sigma_Y$, more typically on the order of $E/30$.

An alternative model of Suo, Shih and Varias (1993), labeled the SSV Model, has been proposed to overcome the above–mentioned limitation of the EPZ Model. In this model, a very thin elastic strip (of sub–micron thickness) is inserted between the extended crack line and the elastic–plastic continuum. This might be thought of as the dislocation–free zone surrounding a crack tip which does not emit dislocations, and Beltz *et al.*, (1996) have extended the model by suggesting a self–consistent procedure for establishing the thickness of the elastic strip. The elastic region surrounding the crack tip allows stresses to reach the levels needed to achieve atomic decohesion. As in the case of the EPZ Model, the SSV Model predicts the relation between Γ_{ss}/Γ_0 and the properties of the outer solid, which is also described as a conventional elastic–plastic continuum. Although stress levels consistent with atomic separation can be achieved, the model nevertheless appears to suffer from significant inaccuracy for the same reason as the EPZ Model does, i.e. conventional plasticity theory is inadequate at the small scales needed to link down to the crack tip, as will now be discussed.

It should not be surprising that conventional continuum plasticity fails to adequately represent behavior all the way down to the scale of the fracture process for such systems. It was developed for application at much larger scales. There is an increasing body of experimental evidence indicating scale effects which give rise to higher elevations of flow stress than can be accounted for by conventional plasticity theory already appear at the scale between 1 to 10 microns (Fleck *et al.*, (1994) and Fleck and Hutchinson (1996)). Nonuniform deformation can produce local hardening which is magnified by factors of 2 or 3 at these scales. We shall end this overview paper with some new results demonstrating the elevation of crack tip stresses predicted by a plasticity theory which incorporates scale dependent hardening. We believe that it is essential to use some such enhanced plasticity model in conjunction with either the EPZ or SSV Model if the link to the fracture process through the plastic zone is to be achieved. The role of discrete dislocations at even smaller scales lying within the continuum plasticity zone is not addressed here. How the dislocation description and the continuum plasticity description will be merged remains unknown.

The continuum theory of strain gradient plasticity theory of Fleck and Hutchinson (1996) postulates that hardening is elevated by both strain and strain gradients. The physical basis of the strain gradient dependence rests on the fact that plastic strain gradients produce geometrically necessary dislocations. When nonuniform deformation takes place at a sufficiently small scale the geometrically necessary dislocations will become dominant. In other words, elevations in effective flow stress will depend on both strain and strain gradients. At large scales, gradient effects are negligible, but they become significant on the scale l. Full details of the strain gradient formulation are given in the article by Fleck and Hutchinson. An effective strain E_e is defined such that

$$E_e = \sqrt{\frac{2}{3}\epsilon'_{ij}\epsilon'_{ij} + l^2\epsilon'_{ij,k}\epsilon'_{ij,k}} \quad (6)$$

where ϵ'_{ij} is the deviatoric strain and $\epsilon'_{ij,k}$ is its gradient. (Complications are omitted here; the precise form of the effective strain and the precise definition of l is given in the cited reference). The effective stress is related to the effective strain by the same power law relation used in the conventional theory $(l = 0)$. Experiments on the torsion of very thin copper wires and indentation experiments on several other metals in addition to copper suggest that 1 is on the order of several microns. It is the sole additional parameter characterizing the solid in the new theory.

Several studies of crack tip fields have been conducted based on the strain gradient theory (Huang *et al.*, 1996; Xia and Hutchinson, 1996). Here, one set of results from Wei and Hutchinson (1996b) have been selected to illustrate the significant effect strain gradients have on the tractions ahead of a crack. The problem is steady–state growth of a mode I crack in a homogeneous solid under plane strain in small scale yielding. The remote field is the elastic field characterized by K_I or, equivalently, by Γ. As before, denote the length quantity which serves as the estimate of the half–height of the plastic zone by R_p, where

$$R_p = \frac{K_I^2}{3\pi\sigma_Y^2} = \frac{E\Gamma}{3\pi(1-\nu^2)\sigma_Y^2} \tag{7}$$

Let x be the distance ahead of the crack tip, and let t_n be the normal traction acting on the extended crack plane directly ahead of the tip. Fig. 8 presents plots of t_n/σ_Y versus x/R_p for three values of $1/R_p$. The parameters specifying the solid are listed in the figure caption. The curve for $1/R_p = 0$ corresponds to the limit for the conventional solid having no strain gradient depen–

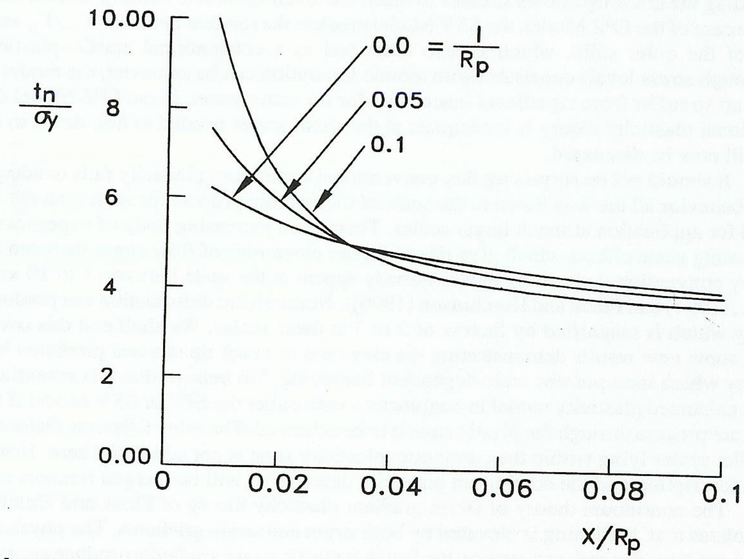

Figure 8. Normal traction acting on the plane ahead of the crack tip for the strain gradient solid (SG solid) of Fleck and Hutchinson (1996) as determined by Wei and Hutchinson (1996b). The crack is a mode I crack propagating in steady–state under plane strain conditions. The case $1/R_p = 0$ corresponds to the limit of a conventional elastic–plastic solid with no strain gradient dependence. The other parameters specifying the solid are $E/\sigma_Y = 300$, $\nu = 0.2$, $N = 0.2$.

dence. This curve is representative of the traction levels that can be attained ahead of a crack tip according to that characterization for a moderately high strain hardening solid $(N = 0.2)$. By contrast, the strain gradient solid with $1/R_p = 0.1$ displays a steep gradient of traction ahead of the tip and has attained a level almost twice that of the conventional solid at $x/R_p = 0.01$. It is expected this traction elevation will have a major effect on the model results of Fig. 3 at the high end of the range of $\hat{\sigma}/\sigma_Y$, were the strain gradient plasticity model to be substituted for conventional plasticity in the formulation of the EPZ Model.

ACKNOWLEDGMENT

This work was supported in part by the National Science Foundation from Grant CMS–9634632, in part by the Office of Naval Research from Grant N00014–96–0559, and in part by the Division of Engineering and Applied Sciences at Harvard University.

REFERENCES

Beltz, G.E., Rice, J.R., Shih, C.F. and Xia, L. (1996). A self–consistent model for cleavage in the presence of plastic flow. *Acta Metall. Mater.* (to be published).

Bilby, B.A., Howard, I.C. and Li, Z.H. (1993). Prediction of the first spinning cylinder test using ductile damage theory. *Fatigue Fract. Engng. Mater. Struct.*, **16**, 1–20.

Broberg, K.B. (1995). Critical review of some methods in nonlinear fracture mechanics. *Eng. Fracture Mech.*, **50**, 157–164.

Brocks, W., Klingbeil, Kunecke, D. and Sun, D.–Z. (1995). Application of the Gurson model to ductile tearing resistance. *Constraint Effects in Fracture: Theory and Applications*, ASTM STP 1244 (ed. M. Kirk and A. Bakker). American Society for Testing Materials, Philadel–phia, PA.

Elssner, G., Korn, D. and Rühle, M. (1994). The influence of interface impurities on fracture energy of UHV diffusion bonded metal–ceramic bicrystals. *Scripta Metall. Mater.*, **31**, 1037–1042.

Fleck, N.A., Muller, G.M., Ashby, M.F. and Hutchinson, J.W. (1994). Strain gradient plasticity: theory and experiment. *Acta Metall. Mater.*, **42**, 475–487.

Fleck, N.A. and Hutchinson, J.W. (1996). Strain gradient plasticity. *Advances in Applied Mech.*, **33** (to be published).

Gurson, A.L. (1977). Continuum theory of ductile rupture by void nucleation and growth: Part I – Yield criteria and flow rules for porous ductile media. *J. Engng. Mater. Technol.*, **99**, 2–15.

Hancock, J.W., Reuter, W.G. and Parks, D.M. (1993). Constraint and toughness parameterized by T. *Constraint Effects in Fracture*, ASTM STP 1171 (ed. E.M. Hackett, K.H. Schwalbe and R.H. Dobbs). American Society for Testing Materials, Philadelphia, PA.

Huang, Y., Zhang, L., Guo, T. and Hwang, K.C. (1996). Near–tip fields for cracks in materials with strain gradient effects. to be published in the Proceedings of The IUTAM Meeting on Non–linear Fracture Problems (ed. J.R. Willis).

Li, Z.H., Bilby, B.A. and Howard, I.C. (1994). A study of the internal parameters of ductile damage theory. *Fatigue Fract. Engng. Mater. Struct.*, **17**, 1075–1087.

Needleman, A. (1987). A continuum model for void nucleation by inclusion debonding. *J. Appl. Mech.*, **54**, 525–531.

Needleman, A. and Tvergaard, V. (1987). An analysis of ductile rupture modes at a crack tip. *J. Mech. Phys. Solids*, **35**, 151–183.

Rousselier, G. (1987). Ductile fracture models and their potential in local approach of fracture. *Nucl. Engng. Design*, **105**, 97–111.

Rousselier, G., Devaux, J.–C., Mottet, G. and Devesa, G. (1989). A methodology for dultile frac–ture analysis based on damage mechanics: an illustration of a local approach of fracture. *Nonlinear Fracture Mechanics: Volume 11–Elastic–Plastic Fracture*, ASTM STP 995 (ed. J. D. Landes, A. Saxena and J.G. Merkle), pp. 332–354. American Society for Testing Mate–rials, Philadelphia, PA.

Shih, C.F. and Xia, L. (1995). Modeling crack growth resistance using computational cells with microstructurally–based length scales. *Constraint Effects in Fracture: Theory and Applications*, ASTM STP 1244 (ed. M. Kirk and A. Bakker). American Society for Testing Materials, Philadelphia, PA.

Sun, D.–Z., Kienzler, R., Voss, B. and Schmitt, W. (1992). Application of micromechanical models to the prediction of ductile fracture. *Fracture Mechanics: Twenty–Second Symposium (Volume II)*, ASTM STP 1131 (ed. S.N. Atluri, J.C. Newman, Jr, I.S. Raju and J.S. Epstein), pp. 368–378. American Society for Testing Materials, Philadelphia, PA.

Suo, Z., Shih, C.F. and Varias, A.G. (1993). A theory for cleavage cracking in the presence of plastic flow. *Acta Metall. Mater.*, **41**, 1551–1557.

Tvergaard, V. and Hutchinson, J.W. (1992). The relation between crack growth resistance and fracture process parameters in elastic–plastic solids. *J. Mech. Phys. Solids*, **40**, 1377–1397.

Tvergaard, V. and Hutchinson, J.W. (1993). The influence of plasticity on mixed mode interface toughness. *J. Mech. Phys. Solids*, **41**, 1119–1135.

Tvergaard, V. and Hutchinson J.W. (1994). Effect of T–stress on mode I crack growth resistance in a ductile solid. *Int. J. Solids Structures*, **31**, 823–833.

Tvergaard, V. and Hutchinson J.W. (1996). Effect of strain–dependent cohesive zone model on predictions of crack growth resistance. *Int. J. Solids Structures*, **33**, 3297–3308.

Tvergaard, V. and Needleman, A. (1984). Analysis of the cup–cone fracture in a round tensile bar. *Acta Metall.*, **32**, 157–169.

Wei, Y. and Hutchinson, J.W. (1996a). Mixed mode interface toughness of metal/ceramic joints. *Mat. Res. Soc. Symp.*, Vol. 409, Material Research Society, 163–170.

Wei, Y. and Hutchinson, J.W. (1996b). Work in progress.

Xia, L. and Shih, C.F. (1995). Ductile crack growth–I. A numerical study using computational cells with microstructurally–based length scales. *J. Mech. Phys. Solids*, **43**, 233–259.

Xia, L. Shih, C.F. and Hutchinson, J.W. (1995). A computational approach to ductile crack growth under large scale yielding conditions. *J. Mech. Phys. Solids*, **43**, 389–430.

Xia, Z.C. and Hutchinson, J.W. (1996). Crack tip fields in strain gradient plasticity. to be published in *J. Mech. Phys. Solids*.